Author(s) Mäkinen, Toni; Pertilä, Pasi; Auranen, Pasi

Title Supersonic bullet state estimation using particle filtering

Citation Mäkinen, T., Pertilä, P. & Auranen, P. 2009. Supersonic bullet state estimation using particle filtering. In: Ming, I.S. (ed.). Proceedings of 2009 IEEE International Conference on Signal and Image Processing Applications, ICSIP, Kuala Lumpur, Malaysia, 18-19 November 2009 6 p.

Year 2009

DOI http://dx.doi.org/10.1109/ICSIPA.2009.5478625

Version Post-print

URN http://URN.fi/ URN:NBN:fi:tty-201306271274

Supersonic Bullet State Estimation Using Particle Filtering

Toni Mäkinen #1, Pasi Pertilä #2, and Pasi Auranen *3

Department of Signal Processing, Tampere University of Technology
P.O. Box 553 Tampere, Finland
1,2 {toni.makinen, pasi.pertila}@tut.fi

* *Savox Communications Ltd*
Vitikka 4 02630 Espoo, Finland
3 pasi.auranen@savox.com

***Abstract*—Due to an increasing number of sniper attacks in different crises and security threats around the world, there is a need for new technologies and applications to take place in helping to prepare against such offensives [1]. Estimation of sound wave direction of arrival (DOA) based on time differences between separate microphones is typically applied for sound source localization, and the existing research achievements of the field are utilized in the presented study. In this paper, a new method for estimating the *state* of a supersonic bullet is proposed. State is defined here to consist of bullet's trajectory, caliber, and speed. The method is based on a mathematical modeling of the bullet shock wave, and the parameter estimation procedure is built over the *Bayesian* inference. Both simulations and real shooting data are used to test and verify the performance of the proposed method. Bringing shock wave modeling and Bayesian inference together is the main focus of the study.**

I. Introduction

In security and peacekeeping it is vital to efficiently estimate the direction of a hostile shooter. Studies have been made in the field of bullet shock waves and trajectory estimation [2], [3], and [4]. In these papers, the mathematical modeling of a shooting event is identical, whereas the methods for detecting waveform signatures and the algorithms for sound source localization differs. Some anti-sniper systems ([5], [6]) are already being used in certain crisis situations, but there still exists a need for improving the reliability of the estimation.

This paper applies a mathematical model of the acoustic waveform of a bullet, that has been studied and measured by Whitman [7]. The previous studies exploit some basic principles of the shock wave signature in the estimation. In contrast, this work applies a *Bayesian approach* to bullet state estimation based on measured data and the mathematical model [7]. The bullet trajectory properties, as well as the caliber and speed, are enclosed by the mentioned bullet state, which is estimated with an inverse Bayesian method. Bayesian method gives an optimal solution in a case where prior knowledge exists. The state estimation problem is of high dimension and the underlying likelihood distribution is highly irregular. *Particle filters* are suitable for such problems [8], and are therefore applied in this work.

Acoustical bullet trajectory estimation methods can be divided into three categories: 1) methods using shock waves, 2) methods using the *muzzle blast* caused by the gun itself, and 3) methods using both of the features. The methods belonging to category 3 have more uncertainty involved in the estimation, since the number of error sources grows higher. Silencers and long shooting distances can prohibit the existence of muzzle blast, causing the category 2 methods to become useless. Nevertheless, they are used in some restless environments in the USA [9]. The proposed method here belongs to category 1, meaning that no observation of the muzzle blast is needed. However, since subsonic bullets do not cause shock waves, only the supersonic bullet states can be estimated. The category 1 methods are still suitable against snipers, who generally prefer rifles yielding supersonic bullets in order to ensure accuracy.

The structure of this paper is the following: First, in Section II the mathematical modeling of a shock wave is reviewed. The following Section III covers the main contribution of the paper: the use of particle filtering to solve the inference problems regarding to the state estimation. In Sections IV and V, the testing and performance of the developed system is covered, and finally conclusions and future work is presented in the last Section VI.

II. Modeling of a Shock Wave

As a bullet propagates in a homogeneous medium at supersonic speed, it creates omni-directionally propagating sound waves, which together form an acoustical shock wave front. As a result, a cone-shaped pattern is formed behind the bullet, see Fig. 1. The angle of the shock wave front with respect to the bullet's trajectory is proportional to the *speed* of the projectile [10]:

$$\theta_M = \arcsin\left(\frac{1}{M}\right), \tag{1}$$

where M is a *Mach number*, which is defined as $M = v/c$, where v and c are the speed of the projectile and sound, respectively.

The waveform of a shock wave is a function of projectile's *diameter* ϕ, *speed* v, and the distance between the trajectory and the receiving microphone position $\mathbf{m}_i$. This *miss distance*

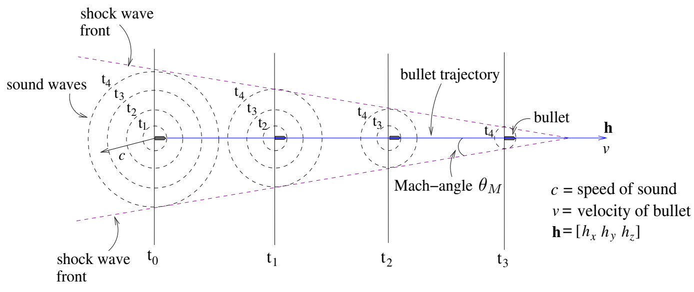

Fig. 1. As a bullet propagates from left to right, a shock wave cone is formed behind the bullet, marked with a purple dashed line. The shock wave front is propagating at the speed of sound c, while the bullet has a decreasing speed, approximated here as a constant v. Vector $\mathbf{h}$ determines the *heading* of the bullet trajectory, whereas the different time indexes are marked by t_n, where n is running from 0 to 4.

is measured from the trajectory's *CPA-point (Closest Point of Approach)*, marked here as $\mathbf{a}$. A line drawn from this point to the microphone position $\mathbf{m}_i$ lies always perpendicular to the trajectory. The shock wave's waveform is mathematically defined using (2) and (3), which form the Whitman model: [7]

$$A_i = \frac{0.53P_0(M^2-1)^{1/8}\phi}{d_{\mathbf{m}_i,\mathbf{a}}^{3/4}l^{1/4}} \text{ [Pa]}, \tag{2}$$

$$L_i = \frac{1.82Md_{\mathbf{m}_i,\mathbf{a}}^{1/4}\phi}{c(M^2-1)^{3/8}l^{1/4}} \text{ [m]}, \tag{3}$$

where P_0 is the atmospheric air pressure, $d_{\mathbf{m}_i,\mathbf{a}}$ is the miss distance, and l is the length of the bullet, which is related to its diameter by [3]

$$l \approx 4.35\phi \text{ [m]}. \tag{4}$$

In addition, the shock wave's time of arrival τ_i to a given microphone $\mathbf{m}_i$ from a specific point $\mathbf{s}$ of the trajectory is needed to model a shock wave caused by a bullet. The term τ_i is defined as

$$\tau_i = \frac{||\mathbf{m}_i - \mathbf{s}||}{c} = \frac{d_{\mathbf{m}_i,\mathbf{s}}}{c} \text{ [s]}, \tag{5}$$

where $d_{\mathbf{m}_i,\mathbf{s}}$ is the distance between the microphone $\mathbf{m}_i$ and the *S-point* $\mathbf{s}$, which is defined in the next Section II-A.

The actual shock wave's waveform is commonly known as *N-shaped* wave (or simply N-wave). This is because the time domain waveform has very dramatic rising and falling edges, which are literally making it to look like a letter "N". This kind of a function can be formed by as is shown in (6), where $\tilde{A}_i$ represents the normalized version of A_i of (2) [2]:

$$y_i(t) = \begin{cases} \tilde{A}_i\left(1 - 2\frac{t-\tau_i}{L}\right), & \tau_i \le t \le \tau_i + L_i \\ 0, & \text{otherwise.} \end{cases} \tag{6}$$

Obviously, the amplitude of the shock wave increases as the miss distance decreases. Also the shock wave length is varying as a function of distance to the trajectory. This can be seen from (3), where the waveform of the shock wave becomes longer, as the trajectory moves further away from

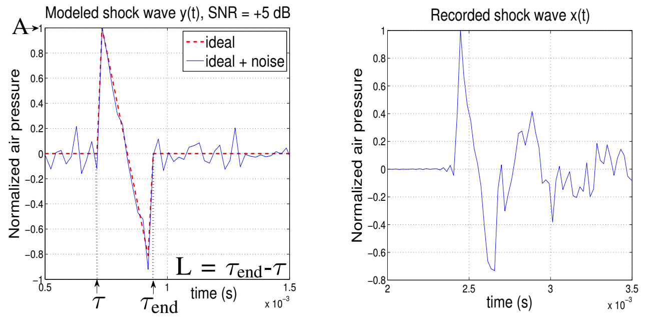

Fig. 2. Modeled and recorded shock waves and the necessary parameters, τ, A and L, for the modeling. Red dashed line on the left image represents an ideal shock wave with zero noise level.

the microphone. In Fig. 2, in the left image, an example of N-wave's waveform with all the necessary parameters can be seen. In order to compare the modeled signal with a real shock wave, also a waveform of a recorded shock wave signal is shown in the right image.

A. Shock Wave's Launching Point

The trajectory's CPA-point differs from the point where the bullet's shock wave is actually launched from, i.e. the S-point. In order to estimate the trajectory of a projectile, the derivation of the CPA-point using the S-point must be obtained — or vice versa. An illustration of the S-point with respect to the CPA is shown in Fig. 3. The blue line represents the line of fire, i.e. the trajectory to be estimated. Vector $\mathbf{g}$ is the *position vector* for the weapon, while vector $\mathbf{h}$ stands for the direction (heading) vector for the bullet. The position vectors are defined in Cartesian coordinates for a particular point, for example $\mathbf{g} = [g_x, g_y, g_z]^T$. *Mach angle* θ_M shown in Fig. 3 is estimated here between the shock wave front and the bullet trajectory. The Mach angle can vary significantly, depending on the speed

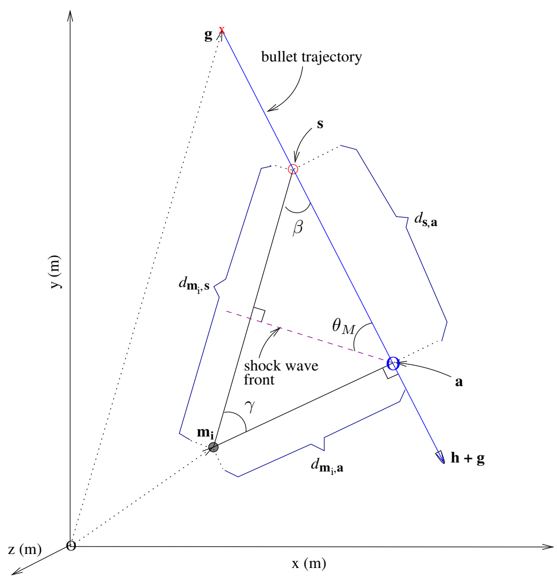

Fig. 3. The geometry of the shock wave front with respect to the CPA - point $\mathbf{a}$ and S-point $\mathbf{s}$. The view of the figure is from above.

of the bullet (1). For bullets that are only slightly faster than the speed of sound, θ_M is nearly $90°$, whereas for very fast bullets, say $v = 1000\ m/s$, θ_M can is as small as $\approx 20°$ [10]. The different angles and metrics of Fig. 3 are obtained by the means of geometry, as will be seen with the simulation in Section IV. As a resulting outcome, the relations between the S-point and CPA can be derived.

III. Estimation of the Bullet's Trajectory

It is assumed that a shock wave — caused by a certain type of a gun and a bullet — has been observed by an *array* of microphones. Furthermore, the coordinates for the microphones are assumed known. An unambiguous direction of arriving (DOA) shock wave can be then calculated, when at least *four* microphones have observed the shock wave. The DOA estimate for the shock wave is based on *time differences* between the shock wave observations of each microphone. With these assumptions, an idea of using *probabilistic inference methods* to estimate the bullet state is proposed.

In Sections III-A and III-B observed data is used to build a so-called *data model*, which is then used to draw conclusions about the unobserved quantities [11]. Here Bayes-methods are considered, since dealing with probability distributions instead of point estimates is a complete solution for the problem.

A. Estimating the Likelihood of a Trajectory

Likelihood function gives *probabilities* for different system outcomes, given that the observed outcome is formed according to some known parameters. It is possible to construct a likelihood function for estimating the probabilities for the observed shock wave *being caused* by a bullet with an arbitrary chosen trajectory, speed and caliber. Likelihood function values are here calculated using a *generalized cross correlation (GCC)* method. The GCC is calculated between the shock wave observations and the modeled shock waves based on (6). The correlation is calculated separately for all the microphones, and a so-called phase transform (PHAT) frequency weighting is also used with the GCC:

$$C_i(t) = \text{IFFT}\left(\frac{X_i Y_i^*}{|X_i||Y_i^*|}\right), \tag{7}$$

where IFFT stands for an inverse Fourier-transform, X_i and Y_i are the Fourier-transforms of the observed and generated shock waves $x_i(t)$ and $y_i(t)$ of microphone channel i, respectively, $(\cdot)^*$ stands for a complex conjugate, $|\cdot|$ is an absolute value, and $C_i(t)$ is the correlation function of microphone channel i at lag t, where t can have values $t \in (-\tau_{max}, \tau_{max})$, τ_{max} being the maximum delay between two microphones. The used phase transform makes the magnitude spectrums of the shock wave signals flat, so that only the phase information is used in calculating the correlation functions [12]. The likelihood value for a bullet state $\mathbf{p}$ is determined by

$$P(\mathbf{p}|\mathbf{O}) = \max\left(\prod_{i=1}^{n} C_i(t)\right), \quad t \in (-\tau_{max}, \tau_{max}) \tag{8}$$

where $\mathbf{O}$ is a $n \times N$ matrix containing the observed signals of length N by n different microphones, and $\mathbf{p}$ is a state vector containing the different parameter values:

$$\mathbf{p} = \left[\mathbf{a}^T,\ \phi,\ v\right]^T. \tag{9}$$

Other methods to determine the likelihood value could also be considered, such as *Mean Square Error (MSE)* between the observed and modeled signals, but here the best results were obtained by using GCC.

In Fig. 4 a outdoor shooting range is shown from above, and the likelihood function of a bullet CPA is plotted on the top by altering the CPA's coordinate. The data used to calculate the likelihood function is taken from the gunshot recordings, discussed in more detail in Section V. The blue areas in Fig. 4 are corresponding to low-probability regions, whereas the dark red color shows the position of the likelihood function's global maximum. The resulting function contains several local maximums and some clutter caused by some non-bullet objects and the background noise. This makes the use of gradient-based search methods difficult. Instead, the particle filters are studied more closely to solve the estimation problem.

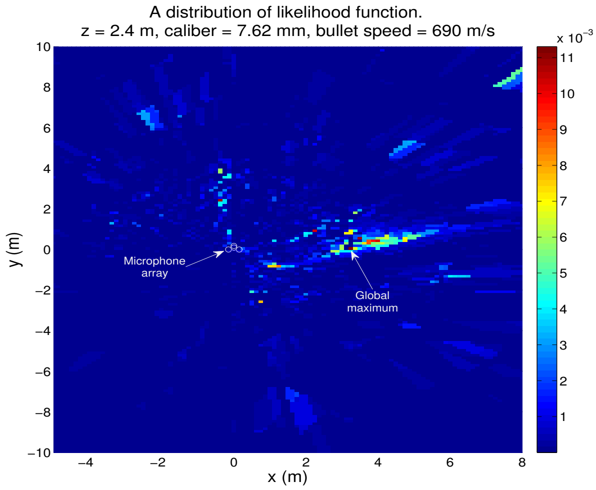

Fig. 4. Likelihood function (Eq. (8)) as a function of x- and y-coordinates of the CPA. The parameters z, ϕ and v are fixed as is described in the title. Four microphones are used in the microphone array.

B. Particle Filter

Particle filter consists of m particles $\mathbf{p}_j$ and weights $W(\mathbf{p}_j)$, where $j = 1, \ldots, m$. Particles represent a "state" of the system to be studied. Particle filters are also known as sequential *Monte Carlo-methods*, and they can be used to numerically estimate the *hidden parameters* or state of the system, based only on the observed data. This is often needed with the inference problems that are too complex to be solved analytically [8].

Since particle filtering is an approximation of Bayesian optimal solution, it follows the Bayes rule (see also (8)):

$$P(\mathbf{O}|\mathbf{p}) \propto P(\mathbf{p}|\mathbf{O})P(\mathbf{O}), \tag{10}$$

where $\propto$ stands for linear proportionality, and $P(\mathbf{O})$ means the *prior* probability distribution assigned to the observations.

Considering the state estimation problem, the functionality of particle filter is bounded to the following process: First, particles are generated to populate the state space based on the a priori information of each parameter: CPA-point is located at radius r from the array, bullet diameter is distributed according to common bullet calibers, and the velocity ranges upwards from the speed of sound. Second, the corresponding shock waves that the microphones *would observe* are generated based on the parameters. After the actual shock wave front has been detected by the used microphone array, i.e. the signals $x_i(t)$ have been received, the process continues by calculating the weight values $W(\mathbf{p}_j)$ for each particle $\mathbf{p}_j$ using (7) and (8). Note that the bullet shock wave must be detected. The detection methods vary, see e.g. [13] and [14] for details. Here the detection stage is omitted for the sake of brevity.

After all the particles are gone through, they are moved randomly in the state space by using here the *Brown's motion*. New weights are calculated and *Metropolis algorithm* is then utilized to update the particles [11]. If a new particle produces a higher weight than the previous one, the upgrading is certain to be done. However, movement towards the lower probability can also occur. The criteria for updating the particles can be mathematically derived by using a random variable α with a uniform distribution over the interval (0, 1). A new particle is then accepted if

$$P(\mathbf{p}_j^\star, \mathbf{p}_j^t) \geq \alpha, \tag{11}$$

where $\mathbf{p}_j^\star$ is the new candidate particle and $\mathbf{p}_j^t$ the particle of the current time index t. Updating is done with the probability

$$P(\mathbf{p}_j^\star, \mathbf{p}_j^t) = \min\left(1, \frac{W(\mathbf{p}_j^\star)}{W(\mathbf{p}_j^t)}\right), \tag{12}$$

where $W(\cdot)$ represents the weight of a corresponding particle, obtained from (8). Equation (12) also shows, that if the update from $\mathbf{p}_j^t$ to $\mathbf{p}_j^\star$ increases the weight, the candidate particle is certain to be kept, that is $\mathbf{p}_j^{t+1} = \mathbf{p}_j^\star$. Metropolis algorithm is a way to avoid converging into a local maximum, since the particles are allowed to move around and to search for the global maximum [11]. Also, in order to prevent the particle filter from converging into any local maximum, 5 % of the particles are randomly distributed again in the state space after each iteration round.

Another very essential concept, called *resampling*, has been developed to help the particles in converging near to the global maximum of the likelihood function. Resampling is used for replacing the particles with low weights with higher weighted ones. This is practically done to avoid the *degeneracy* problem, which can easily occur, if all but one of the particle have weights near zero. In this paper, the systematic resampling is used [8]. After the iterative particle moving, *median* of the resampled particles is taken to represent the output of the particle filter. The iterations are done in total for k times, as is seen in Alg. 1, where the main steps of the proposed procedure are roughly gone through. Because of the orthogonality, the obtained CPA contains all the necessary information to derive the bullet trajectory.

Algorithm 1: A rough algorithm for estimating the CPA.

```
Input: The observed shock wave by each n microphones
Output: Estimated CPA
Initialize the particles according to the prior knowledge.
for iteration ← 1 to k do
    for particle ← 1 to m do
        Derive S-point using the current CPA (sec. II-A).
        for each microphone channel i do
            Model the shock wave addressed by the
            current particle p_j (Eq. (2), (3), (5)).
            Calculate the cross correlation between the
            observed and modeled shock wave (Eq. (7)).
        Multiply the correlation results and take the
        maximum value (Eq. (8)).
        Update p_j using Metropolis algorithm (Eq. (12)).
    Resample p_{1:m} with the resampling algorithm.
p_best ← median{p_{1:m}}.
a ← p_best(1 : 3) .
```

IV. Simulations

For testing the capability of a particle filter to find the global maximum of a likelihood function, a simulation based on the theory of Section II was created. In the simulation, the positions of the gun and each microphone can be determined, along with the bullet's direction, speed and caliber. All of the parameters can be chosen freely, so that the testing environment can be considered as relatively diverse. The distances between the settled microphones and the trajectory are calculated by [15]

$$d_{\mathbf{m}_i,\mathbf{a}} = \frac{||(\mathbf{m_i} - \mathbf{g}) \times \mathbf{h}||}{||\mathbf{h}||}, \tag{13}$$

where $||\mathbf{h}||$ is the norm of vector $\mathbf{h}$, $\times$ represents the cross product of two vectors, and rest of the symbols are described in Section II. Considering again the metrics of Fig. 3, the relations between the CPA and the S-point can be found by solving all the geometric distances. The angle $\beta = 90^\circ - \theta_M$, whereas the terms $d_{\mathbf{m}_i,\mathbf{s}}$ and $d_{\mathbf{s},\mathbf{a}}$ are found as is shown in (14) (using a sine rule):

$$d_{\mathbf{m}_i,\mathbf{s}} = \frac{d_{\mathbf{m}_i,\mathbf{a}}}{\sin\beta}, \qquad d_{\mathbf{s},\mathbf{a}} = \frac{d_{\mathbf{m}_i,\mathbf{a}}\sin\gamma}{\sin\beta}. \tag{14}$$

Now the observations $x_i(t)$ of the shock wave can be modeled according to the chosen simulation settings. Also some Gaussian noise was added to the "observed" signals to test the estimation performance with different *Signal-To-Noise Ratio (SNR)* levels, which are computed for each channel i by

$$\text{SNR}_i = 10\log_{10}\frac{E_{x_i}}{E_{n_i}}, \tag{15}$$

where E_{x_i} and E_{n_i} are the energies of the observed signals $x_i(t)$ and the added noise for each channel, respectively. Energy for signal $x_i(t)$ of length N is calculated by

$$E_{x_i} = \frac{1}{N}\sum_{t=1}^{N} x_i(t)^2. \tag{16}$$

The probability of finding the real likelihood maximum and, unfortunately, the computational burden increases as the number of particles is increased. During the testing it was found out that 2000–3000 particles are enough for the filter to converge in a computational time of about 10 seconds (using Matlab). The number of iterations k was now set to 20, which was decided by following the general progression of the particle weights. The estimation method was tested by generating *four* separate trajectories with a common microphone array located at the origin. The geometrical parameters of the trajectories are shown in Table I. Simulated gunshots were shot 5-7 times along each trajectory, so that in total over 20 estimations were made for each different noise level.

TABLE I
THE USED GEOMETRICAL PARAMETERS IN THE SIMULATIONS.

parameter	x (m)	y (m)	z (m)
$\mathbf{g}_1$	20.000	90.000	1.000
$\mathbf{h}_1$	-60.000	-150.000	0.000
$\mathbf{g}_2$	-15.000	110.000	0.000
$\mathbf{h}_2$	55.000	-150.000	0.000
$\mathbf{g}_3$	15.000	80.000	1.000
$\mathbf{h}_3$	-20.000	-150.000	0.000
$\mathbf{g}_4$	-25.000	80.000	1.000
$\mathbf{h}_4$	20.000	-150.000	0.000
$\mathbf{m}_1$	-0.150	0.000	0.040
$\mathbf{m}_2$	0.149	0.000	0.040
$\mathbf{m}_3$	0.000	0.175	0.040
$\mathbf{m}_4$	0.000	0.094	0.196

The normalized Root-Mean-Square errors (RMSE) of the *averaged S-point estimates* are drawn as a function of SNR in Fig. 5. The RMS error is defined for an observation sequence of length s as

$$\text{RMSE} = \sqrt{\frac{1}{s}\sum_{ind=1}^{s}(\hat{\theta}_{ind} - \theta_{ind})^2}, \tag{17}$$

where $\hat{\theta}$ and θ are the estimated and observed parameter vectors of length s, respectively. Normalization is done here by

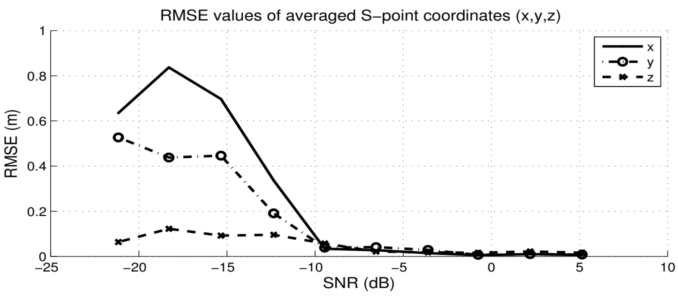

Fig. 5. Normalized RMSE values for the averaged S-point estimates as a function of SNR level.

mapping both the known and the estimated S-point vectors into *unit vectors* before calculating the RMSE values. Hence only the direction of the S-point is considered, which simplifies the comparison between estimation performances at different SNR levels. As the SNR value decreases, the RMS error starts to increase, as one would expect. However, the performance is still good at the SNR level of -8 dB, after which a sudden rise on the error values occur. The results are promising considering the usability of the method in a noisy environment.

V. RESULTS USING REAL-DATA

The simulation does not take into account any non-ideal aspects, such as echo, noise, or wind, which can render the observation circumstances challenging. Moreover, due to the aforementioned facts, the actual observed shock wave form does not perfectly obey the simplified signal model (6), as could be clearly seen in Fig. 2. Therefore, the state estimation procedure was also tested with over a hundred actual shock wave *recordings*, recorded in a outdoor shooting range with a 7.62 mm rifle and two separate microphone arrays with four *Sennheiser MKE 2P-C* condenser microphones attached to both ([16]). Rifle shots were recorded with both arrays at the same time, meaning that the caused shock waves were the same for the both arrays. The shooting sites, as well as the target point, were roughly spatially annotated during the recordings, so that the real bullet trajectory can be kept as more or less known. The microphone positions $\mathbf{m}_i$ are exactly known, and the shock wave observation moments are here manually annotated to avoid false detections and misses.

In Fig. 6, the CPA and S-point estimation results for both the microphone arrays with the recorded 7.62 mm rifle shots can be seen. Totally 114 shots from three different distances (75 m, 50 m, and 25 m) were used. The estimations were done using 2500 particles with 20 iteration rounds, yielding the results with averages μ and standard deviations σ shown in Table II. The average bullet trajectories are plotted with blue dashed lines in Fig. 6, and they are based on the μ results of Table II. The column D on the Table II stands for the estimated miss distance, and it is determined as

$$D = \frac{1}{n}\sum_{i=1}^{n}||\mathbf{m}_i - \mathbf{a}||. \tag{18}$$

The prior knowledge used to initialize the particles is also shown on the last row of Table II. The particle values are kept within these borders during the estimation, e.g. no caliber values less than 2.50 mm are allowed.

TABLE II
THE AVERAGE RESULTS FOR THE CALIBER, BULLET SPEED, AND MISS DISTANCE ESTIMATIONS FOR BOTH ARRAYS.

Array 1	**caliber (mm)**	**speed (m/s)**	**D (m)**
ground truth	7.62	$\approx 670 - 690$	$\approx 3.0 - 7.0$
$\mu \pm \sigma$	6.85 ± 1.31	673 ± 105	11.3 ± 6.0
Array 2	**caliber (mm)**	**speed (m/s)**	**D (m)**
ground truth	7.62	$\approx 670 - 690$	$\approx 16.0 - 20.0$
$\mu \pm \sigma$	7.98 ± 1.14	665 ± 108	16.2 ± 6.8
Priors	$\phi \in (2.50, 12.00)$	$v \in (450, 900)$	$D \in (0.0, 40.0)$

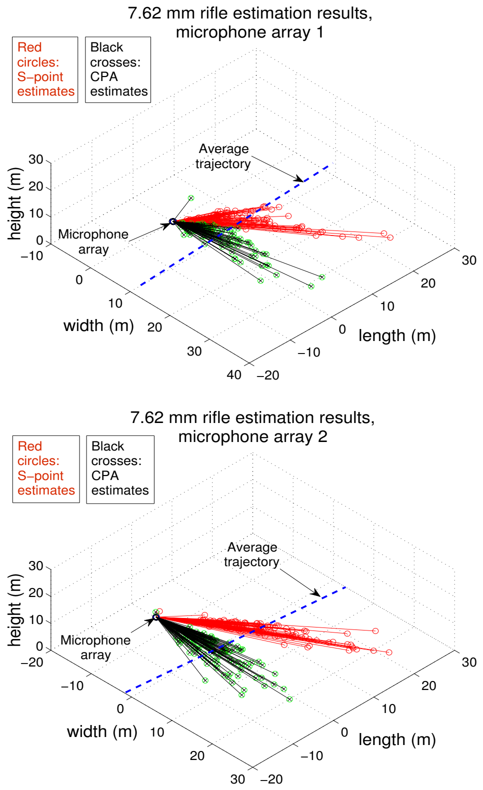

Fig. 6. Estimated CPAs (black crosses) and S-points (red circles) of both microphone arrays for 114 rifle shots. The average bullet trajectories are plotted with blue dashed lines.

In the case of array 1, the miss distance estimates of the nearest 25 m shooting site are too large, which affects also on the overall miss distance result. As the gun is close to the array, the delay between the shock wave and muzzle blast becomes much shorter than with longer shooting distances. The muzzle blast signature can thus easily mix up the estimation, especially since the annotated shock wave observations are not perfect. Due to a rather high amount of separate gunshots, also the standard deviation values are quite high. However, the mean values are approximately correct, as most of the state estimates are concentrated near the ground truth values. It should be yet noted, that the actual trajectory estimation results of Fig. 6 are *not* completely comparable between the two arrays, since the arrays are not sharing exactly the same Cartesian coordinate grid. Nevertheless, it can be stated that the estimation procedure is verified to work with real data.

VI. Conclusions

Using particle filters for trajectory estimation is shown to be working trustworthily with a moderate computational effort. The amount of particles needed in the estimation procedure is scalable, allowing adjustment to be made between the speed and accuracy of the method. Estimations of the bullet caliber and speed are also working relatively well, although the standard deviation can raise rather large, due to misestimated single shots in a longer series.

The proposed estimation approach is shown to be capable to solve the multidimensional inference problem of bullet state estimation. The cross correlation is not dependent on the signal amplitude, which, again, is the most reliable signature for determining the miss distance for the trajectory. Therefore, more research is focused on refining the proposed scheme, as some new recordings with calibrated microphones are planned to be made. Testing the method with correlating noise sources is another future task to be studied.

Acknowledgment

We would like to thank the Finnish Funding Agency for Technology and Innovation (TEKES) for funding (contract 1203/31/07). The data used in the implementation was gathered together with Hasse Sinivaara, Teemu Korhonen and Antti Löytynoja. Hasse Sinivaara also organized the shooting session together with Pasi Auranen, and the original idea of utilizing the shock waves for the estimation was presented by them.

References

[1] N. Shachtman, “Iraq sniper attacks quadruple,” 2007, read 18-May-2009. [Online]. Available: http://blog.wired.com/defense/2007/10/iraq-sniper-att.html

[2] Brian M. Sadler *et al.*, “Optimal and wavelet-based shock wave detection and estimation,” in *J. Acoust. Soc. Am. 104(2)*, August 1998, pp. 955–963.

[3] Brian G. Ferguson *et al.*, “Acoustic sensing of direct and indirect weapon fire,” in *Intelligent Sensors Sensor Networks and Information Processing*, December 2007, pp. 167–172.

[4] P. Volgyesi *et al.*, “Shooter localization and weapon classification with soldier-wearable networked sensors,” in *Proceedings of the 5th International conference on Mobile systems, Applications and Services*, June 2007, pp. 113–126.

[5] BBN Technologies, “Boomerang,” 2009, read 15-April-2009. [Online]. Available: http://www.bbn.com/products_and_services/boomerang/

[6] Areva, “PIVOT system,” 2007, read 26-May-2009. [Online]. Available: http://www.01db-metravib.com/defense.3/news.269/?no_cache=1&L=1

[7] G. Whitman, “The flow pattern of a supersonic projectile,” in *Communications on Pure and Applied Mathematics*, 1952, pp. 301–348.

[8] M. Sanjeev Arulampalam *et al.*, “A tutorial on particle filters for online nonlinear/non-Gaussian Bayesian tracking,” in *IEEE TRANSACTIONS ON SIGNAL PROCESSING, VOL. 50, NO. 2*, February 2002, pp. 174–187.

[9] Edward M. Carapezza *et al.*, “Darpa counter-sniper program: Phase 1 acoustic systems demonstration results,” Edward M. Carapezza and D. Spector, Eds., vol. 2938, no. 1. SPIE, 1997, pp. 299–310.

[10] R. Maher, “Modeling and signal processing of acoustic gunshot recordings,” in *IEEE Signal Processing Society 12th DSP Workshop*, September 2006, pp. 257–261.

[11] A. Gelman *et al.*, *Bayesian Data Analysis*, 2nd ed. CRC Press, 2004, ISBN 1-58488-388-X.

[12] C. Knapp and C. Carter, “The generalized correlation method for estimation of time delay,” in *IEEE TRANSACTIONS ON ACOUSTICS, SPEECH, AND SIGNAL PROCESSING, VOL. ASSP-24, NO 4*, August 1976, pp. 320–327.

[13] T. Chen and H. Wu, “Adaptive impulse detection using center-weighted median filters,” in *IEEE Signal Processing Letters, Vol. 8, No. 1*, January 2001, pp. 1–3.

[14] A. Dufaux *et al.*, “Automatic sound detection and recognition for noisy environment,” in *EUSIPCO 2000: European signal processing conference No. 10*, September 2000, pp. 1033–1036.

[15] E. Weisstein, “Point-line distance – 3-Dimensional,” 2009, read 11-May-2009. [Online]. Available: http://mathworld.wolfram.com/Point-LineDistance3-Dimensional.html

[16] T. Mäkinen, “Detection and direction estimation of impulsive sound sources using a microphone array.” Tampere University of Technology, September 2008, Master of Science Thesis.